BACTOAGAR SULFATE: SYNTHESIS AND PROPERTIES

ALEKSANDR S. KAZACHENKO,[*,**,***] YAROSLAVA D. BEREZHNAYA,[***] YURIY N. MALYAR,[**,***] OLGA YU. FETISOVA,[***] ANTON A. KARACHAROV,[***] TIMUR YU. IVANENKO,[***] NOUREDDINE ISSAOUI,[****] OMAR AL-DOSSARY[*****] and LEDA G. BOUSIAKOU[******]

[*]*Institute of Chemical Technologies, Reshetnev Siberian State University of Science and Technology, Mira st. 82, Krasnoyarsk 660049, Russia*
[**]*School of Non-Ferrous Metals, Siberian Federal University, Pr. Svobodny 79, Krasnoyarsk 660041, Russia*
[***]*Institute of Chemistry and Chemical Technology SB RAS, Federal Research Center, Krasnoyarsk Science Center SB RAS, Akademgorodok 50, bld. 24, Krasnoyarsk 660036, Russia*
[****]*University Monastir, Laboratory of Quantum and Statistical Physics, Monastir, 5079, Tunisia*
[*****]*Department of Physics and Astronomy, College of Science, King Saud University, PO Box 2455, Riyadh 11451, Saudi Arabia*
[******]*IMD Laboratories Co, R&D Section, Lefkippos Technology Park, NCSR Demokritos, PO Box 60037, 15130 Athens, Greece*
✉ *Corresponding author: A. S. Kazachenko, leo_lion_leo@mail.ru*

Received March 26, 2025

This article presents the results of a study of the sulfation of bactoagar with sulfamic acid in the presence of urea. The aim of the work was to study the effect of reaction conditions (temperature and duration) on the yield of the sulfated product and the sulfur content in it. Optimum conditions for sulfation were determined as a temperature of 85–90 °C and a reaction duration of 3 hours, which ensures the maximum yield of the product (92%) and high sulfur content (15.40%). The obtained sulfated samples were analyzed using NMR, FTIR spectroscopy, X-ray diffraction, atomic force microscopy, gel permeation chromatography and thermal analysis. The results of FTIR and NMR spectroscopy confirmed the successful introduction of sulfate groups into the bactoagar macromolecule, and X-ray diffraction showed an increase in the amorphous structure after sulfation. Thermal analysis revealed a decrease in the thermal stability of sulfated bactoagar compared to the original sample. The obtained data demonstrate the potential for the use of sulfated bactoagar in various fields, including biotechnology, pharmacology and drug delivery systems.

Keywords: bactoagar, sulfation, sulfamic acid, urea

INTRODUCTION

Bactoagar is a gel-like nutrient material obtained from seaweeds, which is widely used in microbiology, biotechnology and food industry.[1] Its unique physicochemical properties, such as gelation and high purity, make it an important component in various biological and chemical applications.[2,3] However, in recent years, there has been increased interest in the chemical modification of bactoagar in order to improve its properties and expand the scope of its application.[4,5]

Chemical modification involves changing the chemical structure of natural polymers in order to improve their functional properties. Bactoagar, consisting of agarose and agar, can be modified by various chemical reactions, which allows it to acquire new properties, such as improved strength, resistance to mechanical and thermal stress, as well as specific biocompatibility.[6,7]

Chemical modification of agar can significantly enhance its strength.[8] For example, cross-linking using reagents such as epichlorohydrin can increase the mechanical strength and resistance of the gel to deformation.[9,10]

Modification of agar can significantly improve its biocompatibility, making it suitable for use in medical applications. For example, the introduction of functional groups, such as carboxyl and amino groups, improves cell adhesion. This opens up new horizons for the development of biomaterials, such as tissue compounds.[11]

Agar can also be modified for use in packaging materials that extend the shelf life of products. Studies show that the addition of biopolymers and antimicrobial agents significantly increases shelf life. This can positively affect food safety and reduce waste.[12-14] Modified agar can be used in targeted drug delivery technology.[15,16]

Cell cultures grown on modified agar show improved growth and viability. This opens up new possibilities in the field of regenerative medicine, where cell-cell interactions play a key role.[17,18]

Chemical modification of agar occupies an important place in research and development aimed at improving its physicochemical properties and expanding the areas of application. Progress in this area promises to bring new solutions for various industries, including biotechnology, pharmaceuticals and packaging technologies.[19-21] However, for further successful implementation, it is necessary to continue research aimed at in-depth study of the interactions between modified bactoagar and biological systems.

In this paper, a method for chemical modification of bactoagar with sulfamic acid in 1,4-dioxane in the presence of urea is proposed. The starting materials and their sulfation products were studied by FTIR and NMR spectroscopy, elemental analysis, X-ray diffraction, atomic force microscopy, gel permeation chromatography and thermal analysis.

EXPERIMENTAL

The amounts of sulfamic acid and urea were chosen based on a molar ratio of sulfamic acid to the anhydrogalactose repeat unit of bactoagar (estimated molecular weight per unit ~300 g/mol) of approximately 4:1, assuming the polysaccharide contains free OH groups available for sulfation. Urea was added in a 1:1 molar ratio relative to sulfamic acid, which is typical of the sulfamic acid/urea sulfation system.[22,23] The molarity of the polysaccharide was not directly measured; instead, a fixed mass of air-dried bactoagar (5 g) was used in all experiments, which corresponds to approximately 16.7 mmol of anhydrogalactose units.

Sulfation of bactoagar was carried out with sulfamic acid in 1,4-dioxane in the presence of urea. To do this, 50 mL of dioxane, 6.2 g of sulfamic acid and 3.8 g of urea were placed in a three-neck flask equipped with a thermometer, a mechanical stirrer and a water bath. The resulting mixture was heated with vigorous stirring to 50 °C and 5 g of air-dried polysaccharide was added to it. Then, the temperature and duration of the reaction mixture was raised to a fixed value (in accordance with the sulfation conditions given in Table 1). At the end of sulfation, the solvent was decanted, and the resulting viscous residue was dissolved in 25 mL of water, the excess sulfamic acid was neutralized with a 25% aqueous solution of ammonia until neutral.

The ammonium salt of sulfated polysaccharides was purified by dialysis on cellophane against distilled water. The product was dialyzed for 10 hours, changing the water at intervals of 1-2 hours.

The yield of sulfated bactoagar (reported in Table 1) was calculated as the percentage of the mass of the purified, dialyzed, and freeze-dried product relative to the initial mass of the starting bactoagar used in the reaction (5 g). No correction was made for the mass gain due to the incorporation of sulfate groups; therefore, the reported yields are apparent yields. The sulfur content was determined independently by elemental analysis.

The sulfur content in the obtained pectin sulfates was determined using a Flash EATM-112 elemental analyzer (ThermoQuest, Italy).

FT-IR spectra of the original and sulfated polysaccharide were obtained on a Shimadzu IRTracer-100 IR Fourier spectrometer (Japan) in the wavelength range of 400–4000 cm^{-1}. The spectra were then identified in the OPUS software, version 5.0. Solid samples for IR Fourier analysis in the form of tablets contained 2 mg of substance per 1000 mg of KBr.

X-ray diffraction analysis was carried out on a DRON-3 X-ray diffractometer (monochromatic CuKα radiation, $\lambda = 0.154$ nm) at a voltage of 30 kV and a current of 25 mA. The scanning step was 0.02 degrees, and the intervals were 1 s per data point. The measurements were performed in the range of Bragg angles 2Θ from 5.00 to 70.00°.

The bactoagar and sulfated bactoagar films for AFM imaging were prepared by casting. A 0.1 wt% aqueous solution of each sample was prepared by dissolving the powder in distilled water at 60 °C under stirring for 2 h. A drop (20 μL) of the solution was placed onto a freshly cleaved mica substrate and dried at room temperature under ambient conditions for 24 h, followed by gentle heating at 40 °C for 2 h to remove residual moisture. The resulting films had a thickness of approximately 0.5–1 μm, as estimated by profilometry. The atomic force microscopy measurements of bactoagar film samples and its sulfated derivative were performed on a Solver P47 multimode scanning probe microscope (NT-MDT, Russia) equipped with a 14 μm scanner and an adjustment stage (model SKM). In the semi-contact AFM experiments, silicon rectangular cantilevers (NSG30, NT-MDT, Moscow) with an average resonance frequency of 170 kHz and a force constant of 6 N/m were used. The AFM operating parameters in the semi-contact mode were: scanning speed of 40-55 μm/s, the resolution of the resulting image was 256 x 256 pixels. Scanning was performed in at least 3-4 separate areas on the sample surface. As a rule, smoothing or other image processing, except for the subtraction of the second-order surface, was not performed.

The weight-average molecular weight (Mw), number-average molecular weight (Mn) and polydispersity (PDI) of bactoagar and its sulfated

derivative were determined by gel permeation chromatography using an Agilent 1260 Infinity II Multi-Detector GPC/SEC System chromatograph with a refractometer (RI) as a detector. Separation was performed on combined PL Aquagel-OH 30 and PL Aquagel-OH Mixed-M columns using an aqueous solution of 0.1 M $NaNO_3$ containing 0.025% NaN_3 as a mobile phase. The column was calibrated using polydisperse polyethylene glycol (PEG) standards (Agilent, USA). The eluent feed rate was 1 mL/min, the injected sample volume was 100 μL. Data collection and processing were performed using the Agilent GPC/SEC MDS software.

Thermal analysis was performed using the STA 449 F1 Jupiter instrument (Netzsch, Germany). The thermal degradation of the samples was analyzed in argon in the temperature range from 30 to 700 °C, the flow rate of the protective and purge gases was 20 and 50 mL min^{-1}, respectively. Heating of the samples in the dynamic temperature mode was carried out in corundum crucibles at a rate of 10 °C/min. The measurement results were processed using the software package Netzsch Proteus Thermal Analysis.5.1.0, supplied with the device.

The ^1H NMR spectra were recorded at 25 °C on a Bruker Avance III 600 MHz spectrometer in D_2O. The *zgesgp* pulse sequence from the Bruker library was used to suppress the signal of residual D_2O protons. Chemical shifts are presented relative to the d-solvent signal. All spectra were processed using the Topspin 3.2 software package.

RESULTS AND DISCUSSION

Table 1 presents the results of the study of the effect of reaction conditions on the yield of bactoagar sulfate and its sulfur content. The sulfation process was carried out using sulfamic acid in 1,4-dioxane in the presence of urea. The main parameters varied in the experiment were the temperature and duration of the reaction. The aim of the study was to determine the optimal conditions for maximizing the yield of the product and the sulfur content in bactoagar sulfate.

Table 1
Effect of reaction conditions on the yield of bactoagar sulfate and its sulfur content (sulfation with sulfamic acid in 1,4-dioxane in the presence of urea)

№	Temperature, °C	Time, h	Yield, %	Sulfur content, %
1	90	3	80	15.92
2	85	3	92	15.40
3	95	3	53.6	15.19
4	90	2	59.6	12.69
5	90	4	71.2	15.75

According to the data presented in Table 1, as the temperature increases above 85 °C, the product yield decreases, which is associated with the processes of hydrolysis and thermal degradation of the polymer. The optimum temperature for the maximum yield is in the range of 85–90 °C. The sulfur content reaches a maximum at a temperature of 90 °C, but with a further increase in temperature (up to 95 °C), it begins to decrease. This may be due to the fact that at higher temperatures, partial destruction of sulfate groups occurs.

Increasing the reaction duration from 2 to 3 hours leads to a significant increase in the product yield. However, a further increase in the reaction time to 4 hours leads to a decrease in the yield, which may be associated with the onset of product degradation or side reactions. The sulfur content also rises significantly when the reaction time is extended from 2 to 3 hours. Prolonging the reaction to 4 hours, however, results in only a negligible increase in sulfur content, suggesting that the sulfation limit has been reached. Thus, the optimal conditions for the sulfation process with sulfamic acid in 1,4-dioxane in the presence of urea are a temperature of 85–90 °C and a reaction duration of 3 hours.

The sulfation mechanism in the sulfamic acid/urea system involves the *in situ* formation of sulfamic acid–urea complex, which acts as a sulfating agent. Urea plays a dual role: it activates sulfamic acid by forming a hydrogen-bonded adduct, thereby increasing the electrophilicity of the sulfur atom, and it also buffers the reaction medium, preventing excessive acid-catalyzed hydrolysis of the polysaccharide. 1,4-Dioxane serves as an aprotic solvent that facilitates the swelling of bactoagar and enhances the accessibility of hydroxyl groups for the sulfation reaction. The proposed mechanism is consistent with earlier reports on the sulfation of other polymers using the sulfamic acid/urea system.[23-25]

The obtained bactoagar sulfates were analyzed using a set of physicochemical methods.

The 1H NMR spectrum of native bactoagar contains key signals characteristic of polysaccharides (3.40-4.10 ppm), which correspond to the protons of the carbohydrate rings H2-H6 (Fig. 1). Anomeric H^1 give well-resolved signals at 4.05 and 4.10 ppm. The spectrum of CA-1 shows a noticeable complication at 3.30-4.20 ppm due to the overlapped signals from the modified and original units.

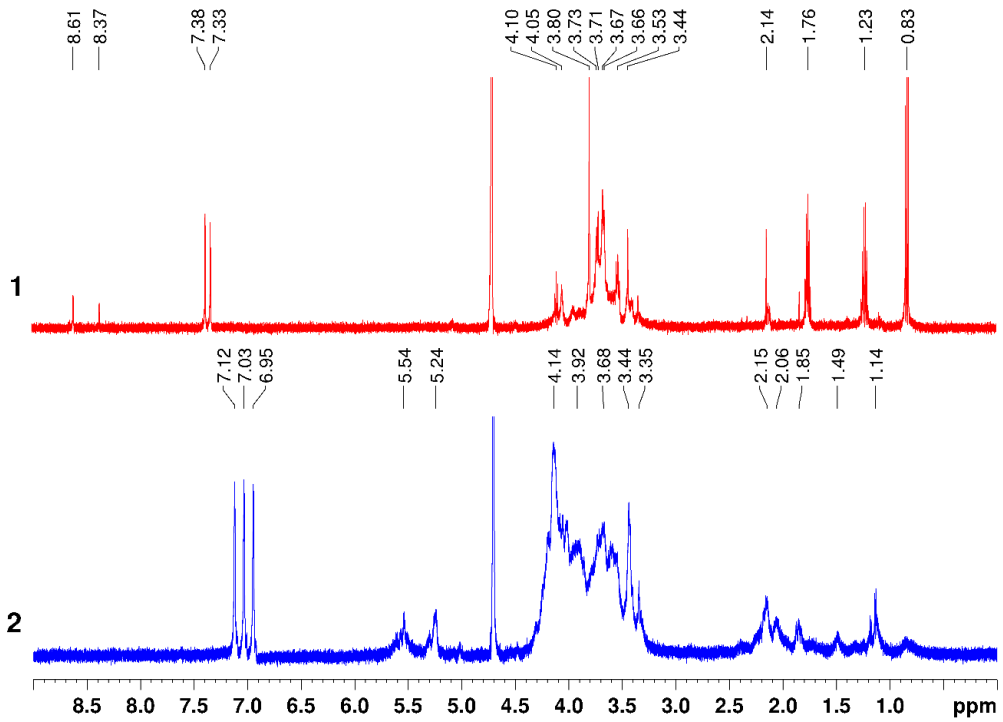

Figure 1: ^{1}H NMR spectra with water suppression of CA-0 (1) and CA-1 (2)

A significant increase of intensity at 4.14 ppm may indicate that it corresponds to a proton that is in similar chemical environments in most units. At the same time, the signals of anomeric H^1 have shifted significantly to a downfield (5.54, 5.24 ppm), which may indicate its proximity to a sulfate group (C2 or C4). The appearance of a series of low-intensity signals at 4.20-4.50 ppm and a triad of signals around 7.0 ppm may relate to CH and OH acetals and/or hemiacetals, indicating partial destruction and oxidation of the sample during the sulfation process.[26,27] The significant downfield shift of the anomeric H^1 signals from 4.05–4.10 ppm in native bactoagar to 5.24 and 5.54 ppm in the sulfated derivative confirms the incorporation of sulfate groups at positions adjacent to the anomeric carbon (most likely at C2 or C4 of the galactose residue). This deshielding effect is typical of protons near an electronegative sulfate substituent. The increased complexity in the 3.30–4.20 ppm region arises from the superposition of signals from non-sulfated and mono-/di-sulfated units. The appearance of low-intensity signals at 4.20–4.50 ppm and around 7.0 ppm suggests the presence of minor degradation products (*e.g.*, reducing ends, formyl groups) formed under the acidic sulfation conditions. Overall, the 1H NMR data corroborate the FTIR and elemental analysis results, confirming successful sulfation, while indicating limited side reactions.

The introduction of a sulfate group into the bactoagar macromolecule was confirmed by IR spectroscopy (Fig. 2). The spectrum of sulfated bactoagar, in comparison with the original (non-sulfated) bactoagar, shows characteristic changes that indicate the successful sulfation process. In the region of 1245–1255 cm^{-1}, a high-intensity absorption band appears, which corresponds to the stretching vibrations of the S=O bonds in the sulfate group. This band is characteristic of the presence of sulfate groups in the molecule.

In the region of 800–821 cm^{-1}, an absorption band is also observed, which is associated with the deformation vibrations of the C-O-S bonds in the

sulfate group. These vibrations confirm the presence of a covalent bond between the carbon of the bactoagar macromolecule and the sulfate group. In the region of 3000–3500 cm^{-1}, a broadening of the absorption band is observed. This is due to the superposition of vibrations of various functional groups, such as: hydroxyl groups (–OH), which are present in the bactoagar structure, ammonium groups ($–NH_4^+$), which can be formed as a result of the interaction of sulfamic acid with urea, CH_2 groups, which are also present in the bactoagar structure.

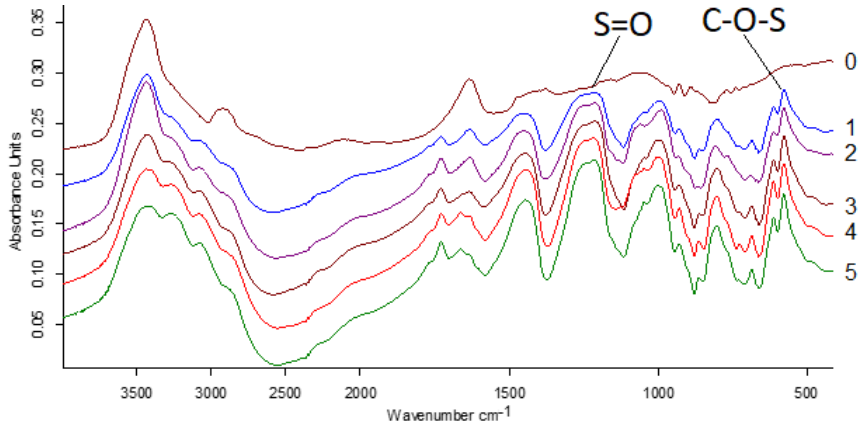

Figure 2: FTIR spectra of: 0 – original bactoagar, 1-5 – sulfated bactoagar (numbering according to Table 1)

The broadening of the band in this region indicates a change in the chemical environment and the interaction between various functional groups after the introduction of sulfate groups. The appearance of absorption bands in the regions of 1245–1255 cm^{-1} and 800–821 cm^{-1} unambiguously confirms the successful introduction of the sulfate group into the bactoagar macromolecule. The broadening of the band in the region of 3000–3500 cm^{-1} indicates complex interactions between hydroxyl, ammonium and CH_2 groups, which may be associated with a change in the structure of the macromolecule after sulfation.

According to the X-ray diffraction data (Fig. 3), the original bactoagar is a non-crystalline (amorphous) substance. This is typical of many polysaccharides, which often do not have a clear crystalline structure due to the complex and disordered structure of their macromolecules.[28,29] The X-ray pattern of the original bactoagar shows a characteristic halo (blurred peak) in the 10–30° 2Θ region, which is a typical sign of the amorphous state of the substance. This halo is due to the lack of long-range order in the arrangement of molecules, which is typical of non-crystalline materials.

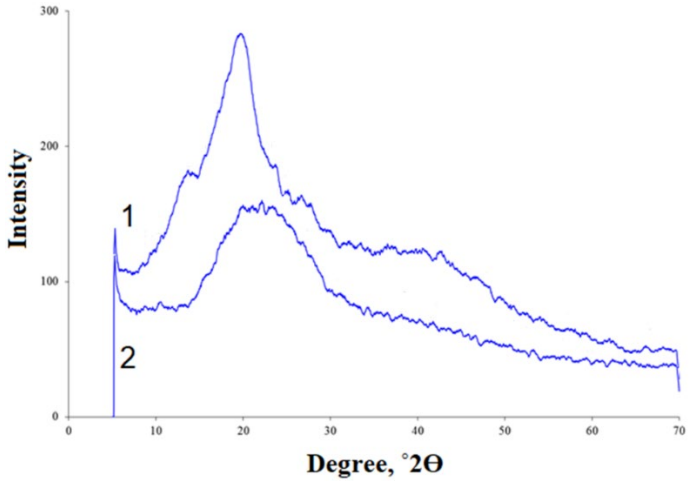

Figure 3: Diffraction patterns of: 1 – original bactoagar, 2 – sulfated bactoagar

During the sulfation process, a decrease in the halo intensity in the 10–30° 2Θ region is observed. This indicates that the bactoagar structure becomes even more amorphous than before modification. The decrease in halo intensity may be due to the fact that the introduction of sulfate groups into the bactoagar macromolecule leads to a disruption of the local order in the polysaccharide structure. Sulfate groups, being bulky and charged, can cause additional deformations and disorder in the molecular structure.[30-32]

The introduction of sulfate groups into the bactoagar macromolecule can lead to a change in intermolecular interactions. Sulfate groups, having high polarity, can disrupt hydrogen bonds and other interactions that could exist in the original bactoagar.[33] In addition, sulfate groups can cause steric hindrance, which leads to an increase in disorder in the polysaccharide structure.[34]

The amorphous state is characteristic of many polysaccharides, such as starch,[35] agarose,[36] and others. However, the introduction of functional groups (for example, sulfate) often leads to further disorder in the structure, which is also observed in the case of bactoagar. The decrease in the halo intensity in the X-ray pattern after sulfation confirms that the modification process leads to an increase in the amorphism of the material. This is due to the introduction of sulfate groups, which disrupt the local order in the polysaccharide structure, increasing the degree of disorder.

The broad halo centered near 22° 2θ in the native bactoagar diffractogram may, in part, arise from residual crystalline cellulose, which is a common impurity in commercial agar products. However, the absence of sharp peaks characteristic of cellulose I or II (*e.g.*, at 14.5°, 16.5°, 22.5°) suggests that cellulose, if present, is in an amorphous or poorly crystalline form and does not dominate the pattern.[37,38] The overall amorphous nature is still the main feature.

According to the AFM data (Fig. 4), the surface of the bactoagar sample is formed by spherical particles with an average diameter of 55 nm. The particles tend to form larger submicron (0.250 μm) aggregates, which gives the surface of the studied sample a rougher structure with the formation of submicron pits in which non-aggregated nanosized particles are concentrated.

Scanning the surface of the bactoagar sulfate sample showed the presence of a thin polymer film on its surface, formed when a drop of an aqueous solution of the sample is dried on the surface. The film covers the entire surface of the sample with an almost uniform layer, smoothing out nanoscale surface inhomogeneities and making it impossible to accurately estimate the diameter of the surface crystallites (according to a rough estimate, their diameter is 80 nm).

For the native bactoagar film, the root-mean-square roughness (Rq) over 5×5 μm areas was 12.3 ± 1.5 nm, with an average particle diameter of 55 ± 8 nm (n = 100). For the sulfated bactoagar film, the apparent Rq decreased to 4.2 ± 0.7 nm due to the smoothing effect of the polymer film formed during drying. The underlying spherical particles in the sulfated sample were estimated to have a diameter of approximately 80 nm.

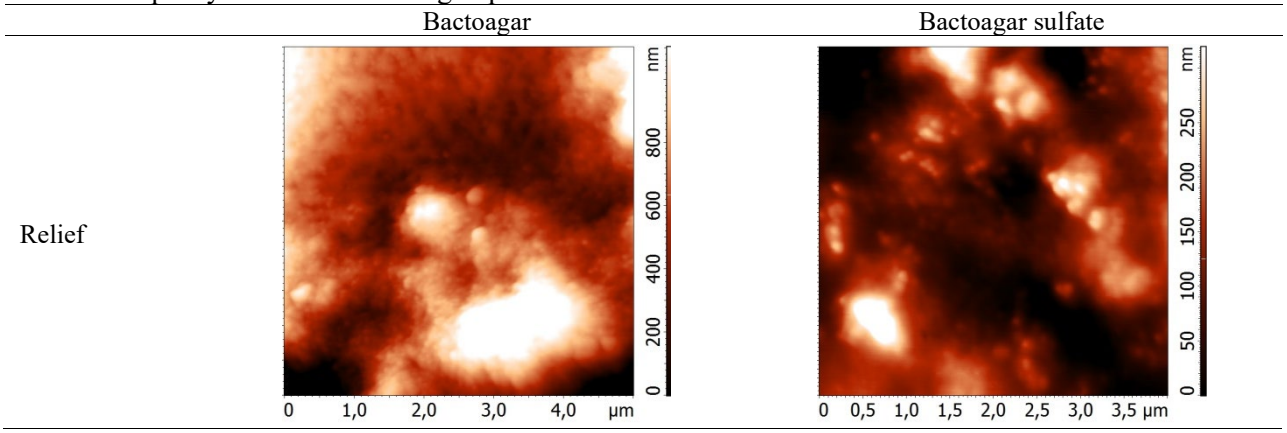

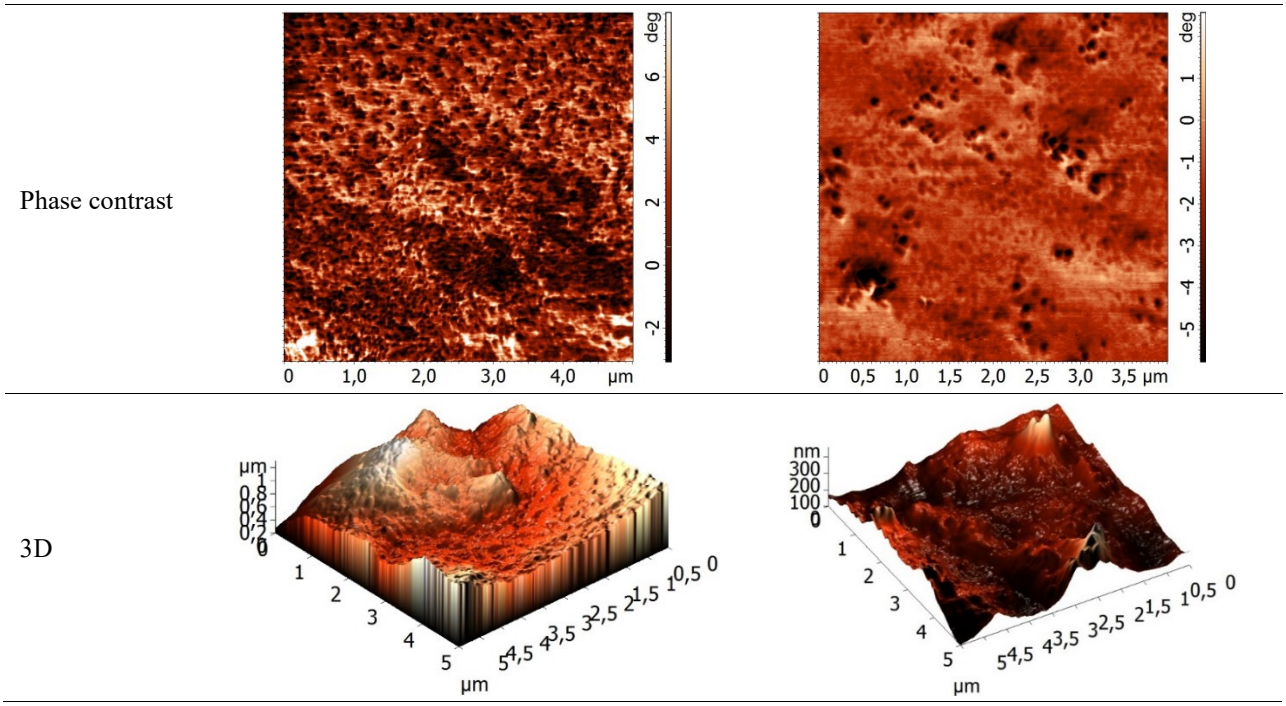

Figure 4: AFM data of the bactoagar samples

The molecular weight distribution curves of native and sulfated bactoagar samples are shown in Figure 5. Native bactoagar is characterized by low solubility in water and tends to form viscous solutions. Therefore, a low concentration of the original bactoagar was used for the study. According to the data obtained, the sample is a set of molecules with a very wide range of molecular weights of $1 \cdot 10^3 \div 1 \cdot 10^6$ with a maximum of about 50 kDa, which is lower than the 120 kDa,[39] or 170-290 kDa,[40] given in the literature. Probably, the increase in average molecular weights is due to DMSO, the eluent used in GPC, which dissolves agarose better. Thus, it can be considered that the MWD of the water-soluble fraction was studied.

In the process of sulfation, due to the addition of ionogenic groups, agarose becomes highly soluble in water, so it becomes possible to obtain higher-quality data on the MWD of the modified sample.

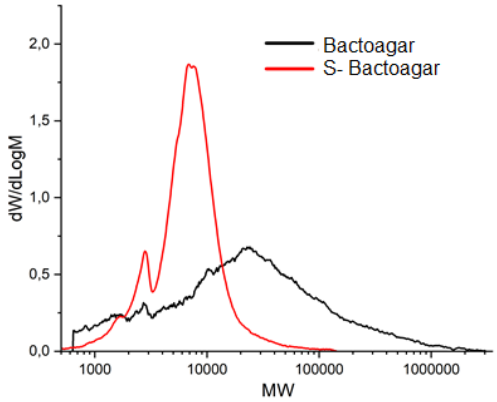

Figure 5: Molecular weight distribution curves of original bactoagar and sulfated bactoagar

Table 2
Molecular weight characteristics of original bactoagar and sulfated bactoagar

Sample	Mn (g/mol)	Mw (g/mol)	PD
Bactoagar	6598	75277	11.41
S-Bactoagar	4933	8456	1.71

According to the GPC data (Fig. 5), strong destruction of agarose chains is observed in the process, which leads to a decrease in the average weight MM by almost 10 times (Table 2). At the same time, the sample becomes more homogeneous with low polydispersity – 1.71. Probably, this is also facilitated by the removal of some low-molecular impurities and polysaccharide degradation products. It is worth noting that the samples obtained in this work differ significantly from those synthesized in an earlier study,[36] using ammonium sulfamate and a wide range of catalysts, which are characterized by less homogeneity. Another difference is the much better solubility of the sample obtained in this work, which may be promising for further use in pharmacology, substance delivery systems, *etc*.

Figures 6, 7 and 8 show the results of thermogravimetric (TG curves), differential thermogravimetric (DTG curves) analysis and differential scanning calorimetry (DSC curves), respectively, of the original (CA-0) and sulfated samples (CA-1).

The data presented in Figures 6 and 7 indicate that the mass loss in the temperature range of 30–700 °C for the initial sample CA-0 occurs in three stages. The DTG curve exhibits two peaks corresponding to the maximum rate of mass loss: 103.5 and 260.2 °C. The first peak corresponds to the removal of adsorption water, which occurs in the range of 30–180 °C. This range on the DSC curve (Fig. 8) is marked by the endothermic effect. The large range of water desorption can be explained by the difficulty of breaking hydrogen bonds between water molecules and polar functional groups of polysaccharides.[41] The decomposition of the main structure of CA-0 begins at 230 °C and up to 400 °C there is an intense mass loss, the sample loses 50% of its mass. In this range, the DTG curve shows a second peak with a maximum at 260 °C, and the DSC curve shows an exothermic peak characteristic of depolymerization reactions of polysaccharide units. After 400 °C, the decomposition intensity decreases, and up to 700 °C, the mass loss was above 10%. The coked residue at the end of thermolysis was 32% of the initial sample.

The modification of the polysaccharide changes its thermal behavior pattern. Judging by the TG and DTG curves (Figs. 6 and 7), the mass loss of the modified sample occurs in four stages. The first stage, as with the initial sample, is associated with water desorption and continues up to 180 °C. The decomposition of sample CA-1 begins at a lower temperature than that of CA-0. Intensive decomposition occurs already at 180 °C, continuing up to 216 °C. On the DTG curve, this stage is marked by a narrow intense peak with a maximum at 199 °C. With further heating, the mass loss continues up to 310 °C. The DTG curve shows a third peak with a maximum at 270 °C.

We assume that the process of the main decomposition starts with the degradation of more accessible and, therefore, more sulfated amorphous regions, while the process at a higher temperature refers to the destruction of the non-sulfated inner part of the compound. During the 2nd and 3rd stages, the modified sample loses 62.2% of its mass. The carbonized residue at the end of thermolysis was 22% of the initial sample. The modification of the CA-0 sample with sulfamic acid significantly reduces the thermal stability, as evidenced by the lower temperature of the onset of decomposition and a smaller residue at the end of pyrolysis of the CA-1 sample.

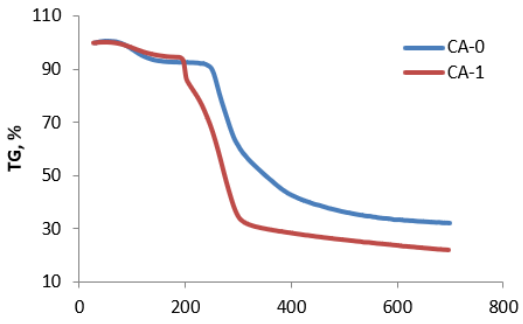

Figure 6: Results of thermogravimetric analysis (TG curves) of samples

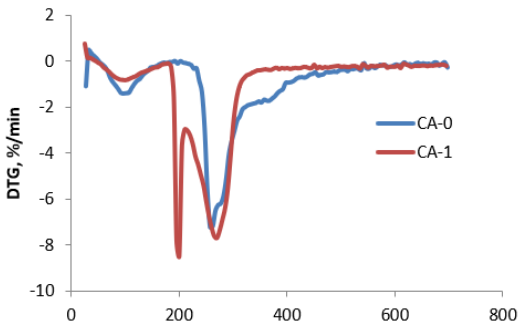

Figure 7: Results of differential thermogravimetric analysis (DTG curves) of samples

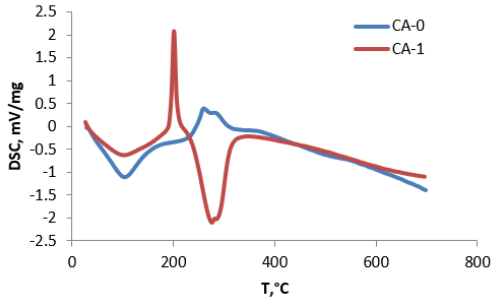

Figure 8: Results of differential scanning calorimetry (DSC curves) of samples

It is important to note that the thermal decomposition of natural polysaccharides and their derivatives involves multiple overlapping reactions (dehydration, depolymerization, charring). Therefore, the activation energy calculated using the Broido method is an apparent value that serves only for comparative purposes within this study, not as an absolute kinetic constant. Nevertheless, this approach is widely used in polysaccharide chemistry to assess relative changes in thermal stability upon chemical modification.[42,43]

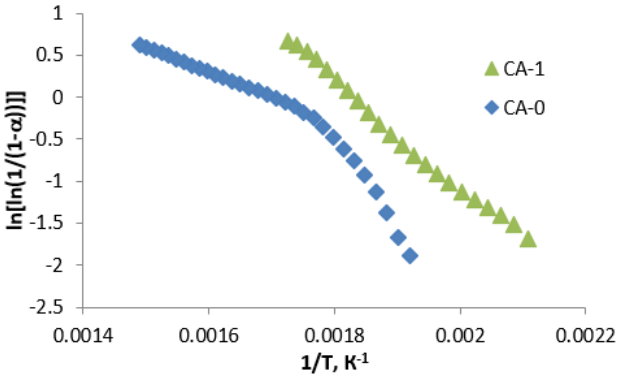

Figure 9: Kinetic curves (Broido plots) for the main stage of thermolysis of CA-0 and CA-1

Table 3
Activation energy values of the main stage of thermal decomposition of samples CA-0 and CA-1

Sample	Temperature range, °C	Activation energy, kJ/mol	R^2
CA-0	248 - 288	95	0.9843
	293 - 398	25	0.9971
CA-1	201-306	53	0.9927

The activation energy (E) of thermal decomposition of the studied substances can be calculated from the TG curve using the Broido equation (1):[44]

$$ln\left[ln\left(\frac{1}{1-\alpha}\right)\right] = -\frac{E}{RT} + ln\left(\frac{ART_m^2}{\beta E}\right) \quad (1)$$

where α is the degree of decomposition of the test sample; E is the activation energy (the calculated value of E for thermal decomposition of natural polymers according to TG curves is, strictly speaking, the "apparent" activation energy, since it corresponds to the simultaneous occurrence of several reactions), J/mol; Tm is the temperature corresponding to the maximum on the DTG curve; A is the frequency factor (s–1), R is the gas constant (8.314 J/mol), and T is the absolute temperature (K); β is the heating rate (deg/min).

From Equation (1), it is evident that the activation energy E is determined by the slope of the straight line constructed in the coordinates $ln\left[ln\left(\frac{1}{1-\alpha}\right)\right]$ from $\frac{1}{T}$.

As shown in Figure 9, the kinetic curve of thermolysis of sample CA-0 has an inflection, which indicates a change in the decomposition mechanism. Unlike the original, the sulfated sample does not change its thermal decomposition mechanism during the main decomposition.

These apparent Ea values should not be overinterpreted as true kinetic parameters. However, the observed decrease from 95 kJ/mol (first stage of CA-0) to 53 kJ/mol (CA-1) consistently indicates that sulfation reduces thermal stability, in agreement with the TG/DTG data (lower onset temperature and lower char residue). The change in the slope for CA-0 (from 95 to 25 kJ/mol) suggests a transition from a more ordered to a less ordered decomposition regime, which is absent in the more amorphous sulfated sample.

The decrease in thermal stability and, consequently, the activation energy of the sulfated polysaccharide occurs as a result of several factors. Firstly, the sulfation of CA-0 ensures the amorphization of its structure, which is confirmed by the results of X-ray phase analysis (Fig. 3). Loose packing contributes to a change in the conformation of macromolecules, which subsequently facilitates the process of thermal decomposition of polymers. Secondly, the sulfated samples of CA-1 have a significantly reduced number of hydroxyl groups (according to FTIR spectroscopy data), which destabilizes intra- and intermolecular hydrogen bonds. During sulfation, available hydroxyl groups are replaced by sulfo-groups, which are more easily cleaved during thermolysis.[42,43]

CONCLUSION

The possibility of sulfation of bactoagar with sulfamic acid in 1,4-dioxane in the presence of urea was demonstrated for the first time. The best results in terms of product yield (92%) and sulfur content (15.40%) were achieved at a temperature of 85–90 °C and a reaction time of 3 hours. Increasing the temperature to 95 °C or reducing the reaction time to 2 hours leads to a decrease in the yield and sulfur content. The IR spectroscopy method confirmed the successful introduction of sulfate groups into the bactoagar macromolecule, which is manifested in the appearance of characteristic absorption bands in the regions of 1245–1255 cm^{-1} and 800–821 cm^{-1}. NMR measurements also confirmed the successful incorporation of sulfate groups, which resulted in a significant downfield shift of the anomeric proton signals (from 4.10 to 5.54 ppm). X-ray diffraction showed an increase in the amorphousness of the structure after sulfation, which is associated with a violation of the local order in the macromolecule. Sulfation leads to significant destruction of agarose chains, which is expressed in a decrease in the average molecular weight by almost 10 times. At the same time, the sample becomes more homogeneous with low polydispersity (1.71). Sulfated bactoagar demonstrates a decrease in heat resistance compared to the original sample. Decomposition begins at a lower temperature, and the residue after pyrolysis is 22% of the initial sample, which is less than that of the original bactoagar (32%). The resulting sulfated samples have improved solubility in water and can be used in various fields, including pharmacology, biotechnology and drug delivery systems. Increased amorphousness and decreased molecular weight can contribute to improved biocompatibility and functional properties of the material.

ACKNOWLEDGMENTS: The work was carried out within the framework of the state assignment of the Institute of Chemistry and Chemical Technology SB RAS (project No. FWES-2026-0011) using the equipment of the Krasnoyarsk Regional Center for Collective Use of the Federal Research Center KSC SB RAS. Part of the study was supported by the Ongoing Research Funging program no. ORF-2026-61, King Saud University, Riyadh, Saudi Arabia.

REFERENCES

[1] P. A. Jaeger, C. McElfresh, L. R. Wong and T. Ideker, *Appl. Environ. Microbiol.*, **81**, 5639 (2015), https://doi.org/10.1128/AEM.01327-15

[2] G. M. Mohamed, A. M. Amer, N. H. Osman, M. Z. Sedikc and M. H. Hussein, *Saudi J. Biol. Sci.*, **28**, 5738 (2021), https://doi.org/10.1016/j.sjbs.2021.06.003

[3] M. Nal, *Biodiversity Int. J.*, **2**, 187 (2018), https://doi.org/10.15406/bij.2018.02.00062

[4] S. Ye, Y. Zhang, J. Chen, F. Chen, H. Weng *et al.*, *Int. J. Biol. Macromol.*, **201**, 364 (2022), https://doi.org/10.1016/j.ijbiomac.2021.12.096

[5] D. Lynam, C. Peterson, R. Maloney, D. Shahriari, A. Garrison *et al.*, *Carbohyd. Polym.*, **103**, 377 (2014), https://doi.org/10.1016/J.CARBPOL.2013.12.069

[6] M. M. A. Sacramento, J. Borges, F. J. S. Correia, R. Calado, J. M. M. Rodrigues *et al.*, *Front. Bioeng. Biotechnol.*, **10**, 1041102 (2022), https://doi.org/10.3389/fbioe.2022.1041102

[7] Y. Li, M. Zhao, L. P. Gomez, R. Senthamaraikannan, R. B. Padamati *et al.*, *Food*

Hydrocoll., **120**, 106905 (2021), https://doi.org/10.1016/J.FOODHYD.2021.106905
[8] B. Qi, S. Yang, Y. Zhao, Y. Wang, X. Yang *et al*., *Gels*, **8**, 162 (2022), https://doi.org/10.3390/gels8030162
[9] Z. Zarei and B. Akhlaghinia, *Chem. Pap*., **69**, 1421 (2015), https://doi.org/10.1515/chempap-2015-0168
[10] S.-Y. Kim and H. Seong, *Colloids Surf. A*, **630**, 127607 (2021), https://doi.org/10.1016/j.colsurfa.2021.127607
[11] F. Jiang, X.-W. Xu, F.-Q. Chen, H.-F. Weng, J. Chen *et al*., *Mar. Drugs*, **21**, 299 (2023), https://doi.org/10.3390/md21050299
[12] F. S. Mostafavi and D. Zaeim, *Int. J. Biol. Macromol*., **159**, 1165 (2020), https://doi.org/10.1016/j.ijbiomac.2020.05.123
[13] V. Hernández, D. Ibarra, J. F. Triana, B. Martínez-Soto, M. Faúndez *et al*., *Materials*, **15**, 3954 (2022), https://doi.org/10.3390/ma15113954
[14] K. Y. Perera, A. K. Jaiswal and S. Jaiswal, *Foods*, **12**, 2422 (2023), https://doi.org/10.3390/foods12122422
[15] M. K. Yazdi, A. Taghizadeh, M. Taghizadeh, F. J. Stadler, M. Farokhi *et al*., *J. Control. Release*, **326**, 523 (2020), https://doi.org/10.1016/j.jconrel.2020.07.028
[16] G. U. Rani, A. K. Konreddy, S. Mishra and G. Sen, *Int. J. Biol. Macromol*., **65**, 375 (2014), https://doi.org/10.1016/j.ijbiomac.2014.01.034
[17] G. Joyce, B. D. Robertson and K. J. Williams, *BMC Res. Notes*, **4**, 73 (2011), https://doi.org/10.1186/1756-0500-4-73
[18] K. Gholami, G. Pourmand, M. Koruji, S. Ashouri and M. Abbasi, *Stem Cell Res. Ther*., **9**, 249 (2018), https://doi.org/10.1186/s13287-018-0997-8
[19] N. E. Montaño, R. D. Villanueva and J. B. Romero, *Dev. Hydrobiol*., **137** (1999), https://doi.org/10.1007/978-94-011-4449-0_67
[20] M. Lahaye and C. Rochas, *Hydrobiologia*, **221**, 137 (1991), https://doi.org/10.1007/BF00028370
[21] A. M. M. Sousa, S. Morais, M. H. Abreu, R. Pereira, I. Sousa-Pinto *et al*., *J. Agric. Food Chem*., **60**, 4977 (2012), https://doi.org/10.1021/jf2053542
[22] A. S. Kazachenko, Y. N. Malyar, N. Y. Vasilyeva, G. N. Bondarenko, I. V. Korolkova *et al*., *Biomass Conv. Bioref*., **12**, 2705 (2022), https://doi.org/10.1007/s13399-020-00855-2
[23] N. Y. Vasil'eva, A. V. Levdansky, B. N. Kuznetsov, G. P. Skvortsova, A. S. Kazachenko *et al*., *Russ. J. Bioorg. Chem*., **41**, 725 (2015), https://doi.org/10.1134/S1068162015070158
[24] B. N. Kuznetsov, N. Y. Vasilyeva, A. S. Kazachenko, V. A. Levdansky, A. A. Kondrasenko *et al*., *Wood Sci. Technol*., **54**, 365 (2020), https://doi.org/10.1007/s00226-020-01157-6
[25] A. S. Kazachenko, Y. N. Malyar, N. Y. Vasilyeva, O. Yu. Fetisova, A. I. Chudina *et al*., *Wood Sci. Technol*., **55**, 1091 (2021), https://doi.org/10.1007/s00226-021-01299-1
[26] A. Serrero, S. Trombotto, P. Cassagnau, Y. Bayon, P. Gravagna *et al*., *Biomacromolecules*, **11**, 1534 (2010), https://doi.org/10.1021/bm1001813
[27] T. Guo, F. Xie and L. Chen, *Int. J. Biol. Macromol*., **277**, 134283 (2024), https://doi.org/10.1016/j.ijbiomac.2024.134283
[28] R. Chandrasekaran, *Adv. Food Nutr. Res*., **42**, 131 (1998), https://doi.org/10.1016/s1043-4526(08)60095-9
[29] E. Atkins, *NATO ASI Ser*., **186** (1990), https://doi.org/10.1007/978-94-009-2129-0_29
[30] A. Martins, C. Alves, J. Silva, S. Pinteus, H. Gaspar *et al*., *Polymers*, **15**, 399 (2023), https://doi.org/10.3390/polym15020399
[31] P. Chen, Y. Xu, S. Yang, Q. Chang, B. Zheng *et al*., *J. Sci. Food Agric*., **101**, 6452 (2021), https://doi.org/10.1002/jsfa.11316
[32] B. N. Kuznetsov, N. Y. Vasilyeva, A. V. Levdansky, A. A. Karacharov, A. S. Krylov *et al*., *Russ. J. Bioorg. Chem*., **43**, 722 (2017), https://doi.org/10.1134/S106816201707010X
[33] M. Duckworth and W. Yaphe, *Carbohyd. Res*., **16**, 189 (1971), https://doi.org/10.1016/S0008-6215(00)86113-3
[34] S. Perez, "Encyclopedia of Biophysics", Springer, Berlin (2013), https://doi.org/10.1007/978-3-642-16712-6_88
[35] F. Akman, A. S. Kazachenko, N. Y. Vasilyeva and Yu. N. Malyar, *J. Mol. Struct*., **1208**, 127899 (2020), https://doi.org/10.1016/j.molstruc.2020.127899
[36] A. S. Kazachenko, N. Y. Vasilyeva, F. Akman, O. Yu. Fetisova, Ya. D. Berezhnaya *et al*., *J. Mol. Struct*., **1294**, 136471 (2023), https://doi.org/10.1016/j.molstruc.2023.136471
[37] S. Selvalakshmi, T. Mathavan, S. Selvasekarapandian and M. Premalatha, *J. Solid State Electrochem*., **23**, 1727 (2019), https://doi.org/10.1007/s10008-019-04262-0
[38] S. Park, J. O. Baker, M. E. Himmel, P. A Parilla and D. K Johnson, *Biotechnol. Biofuels*, **3**, 10 (2010), https://doi.org/10.1186/1754-6834-3-10
[39] R. Armisen and F. Galatas, *FAO Fish. Tech. Pap*., **288**, 1 (1987)
[40] K. Sasuga, T. Yamanashi, S. Nakayama, S. Ono and K. Mikami, *Mar. Biotechnol*., **20**, 520 (2018), https://doi.org/10.1007/s10126-018-9823-7
[41] D. Araújo, T. Rodrigues, C. Roma-Rodrigues, V. D. Alves, A. R. Fernandes *et al*., *Polymers*, **15**, 791 (2023), https://doi.org/10.3390/polym15040791
[42] M. Roman and W. T. Winter, *Biomacromolecules*, **5**, 1671 (2004), https://doi.org/10.1021/bm034519
[43] S. Julien, E. Chornet and R. P. Overend, *J. Anal. Appl. Pyrol*., **27**, 25 (1993), https://doi.org/10.1016/0165-2370(93)80020-Z
[44] A. Broido, *J. Polym. Sci. A*, **7**, 1761 (1969), https://doi.org/10.1002/pol.1969.160071012